

SCALING LAWS FOR FLUXON FORMATION IN ANNULAR JOSEPHSON TUNNEL JUNCTIONS

R. MONACO

*Istituto di Cibernetica del C.N.R, I-80078, Pozzuoli (Na), and
INFN-Dipartimento di Fisica, Universita' di Salerno,
I-84081 Baronissi (Sa), Italy*

AND

R. J. RIVERS

*Blackett Laboratory, Imperial College,
London SW7 2BZ*

1. Scaling Laws for Fluxon Production

1.1. BACKGROUND

Although equilibrium, or adiabatic, correlation lengths $\xi_{ad}(T)$ diverge at the critical temperature T_c of continuous phase transitions, correlation lengths always remain bounded, in practice. This is because causality prevents a system becoming ordered on very large scales within the finite time in which transitions are implemented. In consequence, the order parameter fields become frustrated, and defects arise to mediate between the different equivalent ground states of the system. By observing these defects (in our case, *fluxons*) we obtain a direct experimental guide to the way in which the transition has been implemented.

Causal bounds on defect densities produced in the early universe at GUT transitions were proposed by Kibble[1, 2] but, because of uncertainty in the models, these predictions are not robust. However, Zurek suggested[3, 4] that identical causal arguments were applicable to condensed matter systems, for which direct experiments on defects could be performed.

The reasoning is that, as the temperature $T(t)$ falls through T_c (at time $t = 0$, say), there is a maximum speed $c(t) = c(T(t))$ at which the system can become ordered. Causality suggests that a domain structure, with defects linking domains, cannot be established before time \bar{t} , determined by $|\dot{\xi}_{ad}(\bar{t})| = c(\bar{t})$, the first time at which the rate of collapse of the adia-

batic correlation length is comparable to the maximum permitted speed. For times $t < \bar{t}$ the system is frozen, and \bar{t} measures the first time that we re-enter an adiabatic regime [1, 2, 3, 4]. In appropriate units $\bar{t} = t_0(\tau_Q/\tau_0)^\nu$, where the exponent ν depends on the system, and τ_Q is the quench time.

The second ingredient of the Kibble-Zurek analysis was to identify the defect separation at their time of formation as

$$\bar{\xi} = \xi_{ad}(\bar{t}) = \xi_0(\tau_Q/\tau_0)^\sigma, \quad (1)$$

The value of σ depends on the system, as do ξ_0 and τ_0 . It is this scaling behaviour that we have tested in our experiment, using annular Josephson tunnel junctions (JTJs), for which the defects are *fluxons*.

In fact, the situation is more complex. Defects can only appear with the correct energy profiles when the order parameter has achieved its final state magnitude. This is effected by the exponential growth of unstable modes and is largely completed by the spinodal time t_{sp} , for a transition implemented by phase separation. However, for simple systems it can be shown [5, 6] that, although $t_{sp} > \bar{t}$, $t_{sp} = \bar{t}$, up to $O(1)$ multiplicative logarithmic corrections in τ_Q and the microscopic parameters of the system.

Further, for simple cases, when defects are sheets, tubes or balls of the unstable ground state, the separation of defects is not governed directly by ξ_{ad} , derived from the large-distance behaviour of the field correlator. Rather, it is governed by the separation ξ_{zero} of the field zeroes that label these false groundstates, determined by the short-distance behaviour of the correlation functions. We shall see that this very different understanding of how defects form is crucial for our analysis, when we consider systems of linear size $L < \bar{\xi}$. Nonetheless, the differences between $\xi_{ad}(\bar{t})$ and $\xi_{zero}(t_{sp})$ still remain logarithmic in τ_Q , and the simple scaling behaviour (1) is reliable at the level of accuracy of the experiments [7, 8, 9, 10, 11, 12, 13] that, prior to ours, have been performed to check it.

1.2. THE SCALING PREDICTIONS FOR FLUXONS

The order parameter of a Josephson tunnel junction at temperature $T < T_c$ is the phase difference ϕ of the macroscopic superconducting quantum mechanical wave functions across the barrier. For an annular JTJ (AJTJ) with a bias current Γ , ϕ obeys [14] the perturbed Sine-Gordon equation

$$\frac{\partial^2 \phi}{\partial x^2} - \frac{1}{c^2(T)} \frac{\partial^2 \phi}{\partial t^2} - \frac{1}{\lambda_J^2(T)} \sin \phi = \Gamma + \frac{\alpha}{c^2(T)} \frac{\partial \phi}{\partial t} - \beta \frac{\partial^3 \phi}{\partial x^2 \partial t} \quad (2)$$

provided the width Δr of the annulus, of radius r , satisfies $\Delta r \ll r$ and $\Delta r \ll \lambda_J(T)$, the Josephson coherence length; x measures the distance along the annulus, $c(T)$ is the Swihart velocity, and α and β are the

coefficients of the losses due to the tunneling current and to the surface impedance, respectively.

The boundary conditions for Eq.(2) are periodic, $\phi(x+C) = \phi(x) + 2\pi n$, where $C = 2\pi r$ is the circumference of the junction and the winding number n is an integer corresponding to the algebraic sum of fluxons trapped in the junction barrier at the normal-superconducting (N-S) transition.

The classical fluxons are the 'kinks' of the Sine-Gordon theory. Eq. (2) is only valid once the transition is complete, and we shall not use it to study the appearance of fluxons. However, it is sufficient to enable us to identify $\lambda_J(T)$, diverging at T_c , as the equilibrium correlation length $\xi_{ad}(T)$ to be constrained by causality. Further, the Swihart velocity $c(T)$ measures the maximum speed at which the order parameter can change[15, 16].

For the experiment that we shall describe below, we find that $C < \bar{\xi}$. In fact, because we are really counting field zeroes (mod 2π), the conclusions are equally valid for small systems. Any field crossing zero (mod 2π) has the potential to mature into a fluxon. Thus, before the causal time we have a picture in which there is a fractal thermal fuzz of potential fluxons, whose density depends on the scale at which we look. By $O(\bar{t})$ some of these have developed into the fluxons that we see subsequently (see [5, 6]). However, because from this viewpoint we have many proto-defects jockeying to become the real thing, the relevant scale to compare to the system size is not $\bar{\xi}$ but ξ_0 , and $C \gg \xi_0$.

A detailed discussion of JTJs has been given elsewhere by us [17, 18], including a summary of this experiment [19], and we refer the reader to these articles for more details. The JTJs in our experiment are *symmetric*, i.e. the electrodes are made of identical superconducting material. For such JTJs $\nu = 1/2$ and $\sigma = 1/4$. Therefore, at the time of their formation the separation of fluxons is expected to be

$$\bar{\xi} \sim \xi_0(\tau_Q/\tau_0)^{1/4}. \quad (3)$$

In terms of the parameters of the JTJs, $\xi_0 = \sqrt{\hbar/2e\mu_0 d_s a J_c(0)}$, where $J_c(T)$ is the critical Josephson current at temperature T for a JTJ with superconductors with effective thickness d_s . The parameter a is given in terms of the gap energy and critical temperature and has a value between 3 and 5. As for τ_0 , it is given as $\tau_0 = \xi_0/c_0$, where c_0 defines the behavior $c(t) = c_0(t/\tau_Q)^{1/2}$ of the Swihart velocity for the system near $T = T_c$.

2. The Experiment

2.1. MEASURING FLUXONS

When fluxons are produced they are static. To see them it is necessary to feed a bias current to the AJTJ, whereupon they move as magnetic dipoles.

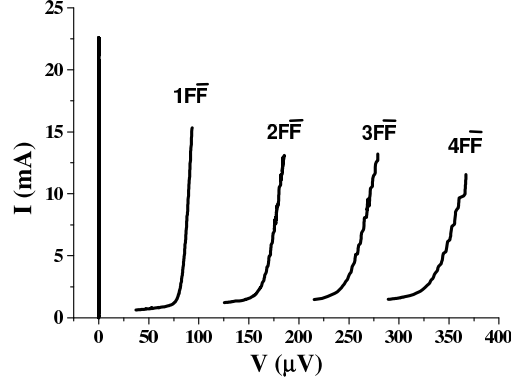


Figure 1. The measured current-voltage characteristics of an AJTJ without trapped fluxons. For each current branch the number of fluxon-antifluxon pairs $F\bar{F}$ is indicated.

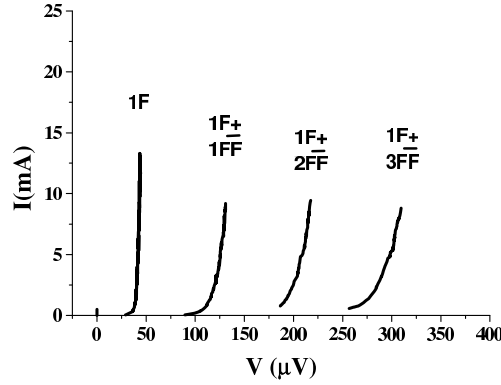


Figure 2. The current-voltage characteristics of the same annular JTJ as in Fig.1 with one trapped fluxon and fluxon-antifluxon pairs.

As a result, they leave a clear signature on the junction current-voltage characteristic (IVC). Fluxons having different topological charge $n = \pm 1$ travel in opposite directions. Quantitatively, if a fluxon travels around an AJTJ having circumference C with a constant speed $v < c(T)$, then an average voltage $V = \Phi_0 v / C$ develops across the junction. By changing the bias current through the barrier the voltage drop changes and a new branch appears on the junction IVC. When N fluxons travel around an AJTJ, the junction voltage is $V = N\Phi_0 C / v$. In this expression N is the total number of travelling fluxons and can be larger than the winding number n if $F\bar{F}$ pairs are travelling around the annulus. Therefore, we can count the number of travelling fluxons by simply measuring the voltage across the AJTJ.

To show this, Figs.1 and 2 represent the IVC of the same AJTJ with no fluxon trapped and with one fluxon trapped, respectively. We note

that with no trapped fluxons the zero voltage current is very large. In the other case the supercurrent is rather small (ideally zero) and large current branches can be observed at finite voltages corresponding to the fluxon and, possibly, $F\bar{F}$ pairs travelling around the junction.

2.2. THE EXPERIMENTAL SETUP

High quality $Nb/Al-Al_{ox}/Nb$ JTJs were fabricated on 0.5 mm thick silicon substrates (chips) using the trilayer technique described in Ref.[22]. Each JTJ had a mean circumference $C = 500\ \mu\text{m}$ and a width $\Delta r = 4\ \mu\text{m}$. The thicknesses of the base, top and wiring layer were 200 , 80 and $400\ \text{nm}$, respectively. The high quality of the samples was inferred from the I-V characteristic at $T = 4.2\ \text{K}$ by checking that the subgap current I_{sg} at $2\ \text{mV}$ was small compared to the current rise ΔI_g in the quasiparticle current at the gap voltage V_g .

The symmetry of the junctions is assured by the absence of a logarithmic singularity in the IVCs at low voltages and the linear temperature dependence of the critical current as the temperature T approached the critical temperature T_C . Many samples have been measured. For clarity only two will be discussed here. Their geometrical and electrical (at $4.2\ \text{K}$) parameters of are listed in Table I. In particular, they differ in their critical current densities. The Swihart velocity c_0 has the value $c_0 = 1.4 \times 10^7\ \text{m/sec}$.

TABLE 1. The samples

Sample	A	B
Mean circumference $C(\mu\text{m})$	500	500
Width $\Delta r(\mu\text{m})$	4	4
Zero field critical current $I_o(\text{mA})$	33	2.5
Maximum critical current $I_{\text{max}}(\text{mA})$	39	2.7
Gap quasiparticle current step $\Delta I_g(\text{mA})$	88	5.2
$I_{\text{max}}/\Delta I_g$	0.45	0.52
Critical current density $J_c(\text{A/cm}^2)$	3050	180
Josephson length $\lambda_J(\mu\text{m})$	6.9	28
Normalized mean circumference C/λ_J	72	18
Quality factor $V_m(\text{mV})$	49	63
Normal resistance $R_N(\text{m}\Omega)$	36	610
ZFS1 asymptotic voltage (μV)	51	53

In order to vary the quenching time in the broadest possible range, we have realized the experimental setup schematically shown in Fig.3. A massive Cu block held to the sample holder was used to increase the system

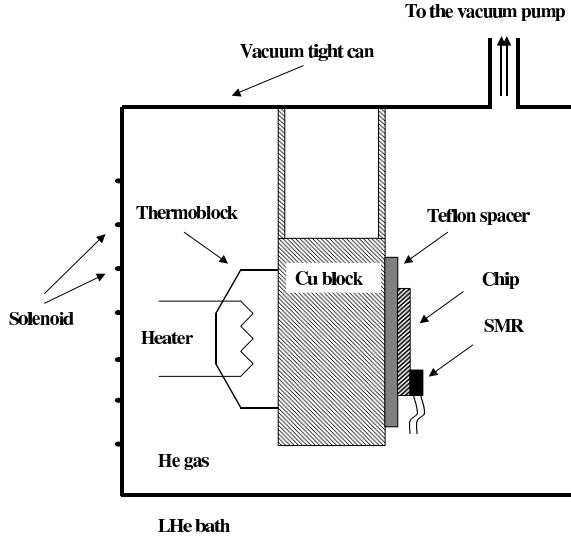


Figure 3. Sketch (not to scale) of the cryogenic insert developed to perform the junction thermal cycles over slow and fast timescales

thermal capacity. The chip was mounted on one side of this block. On the other side, a thermoblock was mounted consisting of a $50\ \Omega$ carbon resistor and two thermometers in order to measure and to, if necessary, stabilize the Cu block temperature. Finally a small sized $100\ \Omega$ surface mounted resistor (SMR), was kept in good thermal contact with the chip.

This system allowed us to perform the sample quenching over two quite different time scales. By means of the resistor in the thermoblock, a long time scale was achieved by heating the chip through the Cu block; on the contrary, a short current pulse through the SMR on the chip, attained much short thermal cycles. The total system was kept in a vacuum-tight can immersed in the LHe bath at He gas pipeline pressure. By changing the exchange gas pressure and using the two techniques, the quenching time can be changed over a quite large range from tenths to tens of seconds.

The temperature dependence of the junction gap voltage was exploited to monitor the temperature of the junction itself during the thermal cycle. The analytical expression [20] for the superconductor gap energy $\Delta(T)$,

$$\frac{\Delta(T)}{\Delta(0)} = \tanh \frac{\Delta(T) T_c}{\Delta(0) T}, \quad (4)$$

also applies to the junction gap voltage that is proportional to it. In this way we derive temperature profiles for slow and fast cycles, assuming for $\Delta(0)$ and T_c the values $2.85\ meV$ and $8.95\ K$, respectively, as found by Monaco *et al.* [21] on similar JTJs.

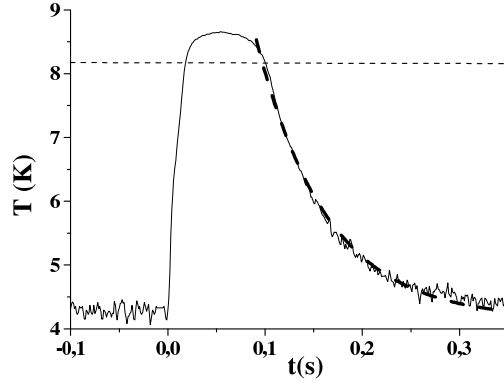


Figure 4. Time dependence of the junction temperature (only reliable below the horizontal dashed line) during a slow thermal cycle, as determined from (4). The thick dashed line is the best fitting curve to (5).

We are only interested to the cooling process, and we use (4) to fit our data by a simple thermal relaxation equation:

$$T(t) = T_{fin} + (T_{in} - T_{fin}) \exp\left(-\frac{t - t_0}{\tau}\right) \quad (5)$$

with only two fitting parameters t_0 and τ , and T_{in} and T_{fin} fixed at 8.95 and 4.15 K, respectively. In Eq.5 t_0 is the time at which $T = T_{in} = T_c$ and τ is the relaxation time which sets the cooling time scale. The fitting curve for a fast quench is shown by a thick dashed line in Fig.4, corresponding to a thermal relaxation time τ of 0.073 s. The dashed horizontal line indicates the temperature threshold below which the temperature time dependence can be reliably accounted for by our measured data. The quenching time τ_Q can be obtained from its definition $\tau_Q = -T_C/\dot{T}$ at $T = T_C$, giving $\tau_Q = \tau T_C/(T_{in} - T_{fin})$.

2.3. THE MEASUREMENTS

Quenching experiments were carried out in a double μ -metal shielded cryostat and the transitions from the normal to the superconducting states were performed with no current flowing in the heaters and the thermometers. Both the junction voltage and current leads were shorted during the all thermal cycle. Furthermore, the heat supplied to the sample was such that the maximum temperature reached by the junction was made slightly larger than its critical temperature, say at about 10 K, in order to make sure that also the bulk electrode critical temperature ($T_C \simeq 9.2K$) was exceeded. In this case, according to Eq.5, the value of the quenching time is $\tau_Q \simeq 1.7 \tau$. The value of the quenching times has been determined to an

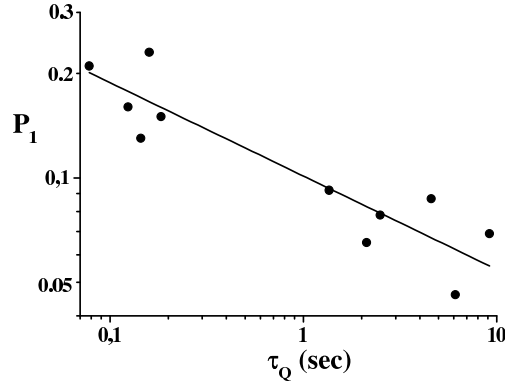


Figure 5. Log-log plot of the probability P_1 to trap one fluxon versus τ_Q . The solid line is the best fitting curve, assuming a power law dependence as in (1).

overall accuracy of better than 5%. For each value of the quenching time, in order to estimate the trapping probability, we have carried out a set of 300 thermal cycles and at the end of each cycle the junction IVC was inspected in order to ascertain the possible spontaneous trapping of one or more fluxons.

As we shall see later, the AJTJs are such that the ZK causal length $\bar{\xi} > C$ by roughly an order of magnitude. Thus the probability of finding a single fluxon is small. In the following we will focus our attention only on the probability P_1 to trap just one fluxon, although a few times we found clear evidence of two and, more seldom, three homopolar fluxons spontaneously trapped during the N-S transition. However, these events were too rare to be statistically significant. Experimentally, we define P_1 as the fraction of times in which at the end of the thermal cycle the junction IVC looks like Fig.1b, i.e. with a tiny critical current and a large first ZFS. Our definition of P_1 is reasonable as far as the chance to trap two fluxons is negligible.

3. The results

When $\bar{\xi} > C$ we estimate the probability of finding a fluxon in a single quench to be

$$P_1 \simeq \frac{C}{\bar{\xi}} = \frac{C}{\xi_0} \left(\frac{\tau_Q}{\tau_0} \right)^{-\sigma}, \quad (6)$$

where, from (3), $\sigma = 0.25$.

Fig.5 shows on a log-log plot the measured probability P_1 of a single fluxon trapping obtained by quenching the sample A 300 times for each value of the quenching time τ_Q changed by varying the exchange gas pressure and by using both the fast and slow quenching techniques. Although

the points are quite scattered, we attempted to fit the data with an allometric function $P_1 = a \cdot \tau_Q^{-b}$ with a and b being free fitting parameters. We found that the best fitting curve, shown by the solid line in Fig.6, has a slope $b = 0.27 \pm 0.05$. Such a value of b , although affected by a 20% uncertainty, is in good agreement with the expected $b = 0.25$ dependence.

For the coefficient a we found the best fitting value of $0.1 \pm 10\%$ (τ_Q in seconds). This is to be compared with the predicted value of $C\tau_0^{1/4}/\xi_0$. Sample *A* had a circumference $C = 500 \mu m$. Its effective superconductor thickness was $d_s \approx 250 nm$. At the final temperature $T_{fin} = 4.2 K$, the critical current density was $J_c(T_{fin}) = 3050 A/cm^2$ and the Josephson length was $\lambda_J(T_{fin}) = 6.9 \mu m$. From this, and c_0 given earlier, we infer that $\xi_0 \approx 3.8 \mu m$ and $\tau_0 \approx 0.17 ps$. This then gives $C\tau_0^{1/4}/\xi_0 \approx 0.08 s^{1/4}$, in good agreement with the experimental value of a , given the fact that we only expect agreement in overall normalization to somewhat better than an order of magnitude level.

Similar measurements have been carried out for sample *B*. Although compatible with (3), the results were affected by a data scattering even larger than that found for sample *A*. This is due to a much smaller normalized length which, according to (6), translates in a expected probability P_1 , for a given τ_Q , about four times smaller, far too small to get statistically significant data in reasonable times. However the roughly measured probability P_1 of 1 fluxon every 50-100 attempts is in fairly good agreement with the expected value.

4. Comments, Future Experiments and Conclusions

We consider this experiment to give a striking confirmation of the Zurek-Kibble predictions.

Of the several experiments [7-13] that had been performed prior to ours to test (1) only two [12, 13] had variable τ_Q and could confirm scaling behaviour. Of these, only one experiment [13] shows KZ scaling. Given this relatively poor success rate in confirming (3) we are considering a further experiment to measure the ZK scaling exponent, this time with manifestly non-symmetric AJTJs, which require different fabrication techniques. In this case the value of σ inferred from the same causal arguments is $\sigma = 1/7$, very different from the $\sigma = 1/4$ that we tested above.

Our experiments have demonstrated that quenching times of the order of 1 second give a rather large probability to trap one fluxons on AJTJs having a very large normalized length. However, very long junctions mean very large critical current densities that, in turn, require Josephson barriers so thin that their quality and uniformity is often spoiled. For these reasons, it would be highly desirable to compensate the reduced junction length

with an increased quenching rate, as it is suggested by the findings for sample *B*. On the contrary, in order to lower the quenching time, it is necessary to resort to new techniques since the maximum power that can be dissipated by the surface mount resistors sets an obvious lower threshold on τ_Q . One possible way to reach this goal is to perform the junction thermal cycle by means of light pulses. Light dissipates inside the superconducting electrodes, but not in the substrate providing a local junction heating that will relax much faster to the background temperature. We estimate that, by using a properly focussed pulsed light beam, the quenching time scale can be reduced to the μs range.

Acknowledgements

The authors thank J. Mygind for invaluable help in conducting the experiment and L. Filippenko for the sample fabrication.

References

1. T.W.B. Kibble, *J. Phys.* **A9**, 1387 (1976).
2. T.W.B. Kibble, *Physics Reports* **67**, 183 (1980).
3. W.H. Zurek, *Nature* **317**, 505 (1985), *Acta Physica Polonica* **B24**, 1301 (1993).
4. W.H. Zurek, *Physics Reports* **276**, Number 4, Nov. 1996.
5. E. Kavoussanaki, R.J. Rivers and G. Karra, *Cond. Matt. Phys.* **3**, 133 (2000).
6. R.J. Rivers, *Journal of Low Temperature Physics* **124**, 41 (2001).
7. V.M.H. Ruutu *et al.*, *Nature* **382**, 334 (1996).
8. C. Bauerle *et al.*, *Nature* **382**, 332 (1996).
9. P.C. Hendry *et al.*, *Nature* **368**, 315 (1994).
10. M.E. Dodd *et al.*, *Phys. Rev. Lett.* **81**, 3703 (1998), *J. Low Temp. Physics* **15**, 89 (1999).
11. R. Carmi and E. Polturak, *Phys. Rev.* **B 60**, 7595 (1999).
12. S. Casado, W. González-Viñas, H. Mancini and S. Boccaletti, *Phys. Rev.* **E63**, 057301 (2001).
13. S. Ducci, P.L. Ramazza, W. González-Viñas, and F.T. Arecchi, *Phys. Rev. Lett.* **83**, 5210 (1999).
14. N. Grønbech-Jensen, P. S. Lomdahl, M. R. Samuelsen, *Phys. Lett. A* **154**, 14 (1991).
15. J.C. Swihart, *J. Appl. Phys.*, **32**, 461 (1961).
16. A. Barone and G. Paterno, *Physics and Applications of the Josephson Effect*, John Wiley & Sons, New York (1982).
17. E. Kavoussanaki, R. Monaco and R.J. Rivers, *Phys. Rev. Lett.* **81**, 3452 (2000).
18. R. Monaco, R.J. Rivers and E. Kavoussanaki, *Journal of Low Temperature Physics* **124**, 85 (2001).
19. R. Monaco, J. Mygind and R.J. Rivers, *Phys. Rev. Lett.* **89**, 080603 (2002)
20. D.J. Thouless, *Phys.Rev.* **117**, 1256 (1960).
21. R. Monaco, R. Cristiano, L. Frunzio, C. Nappi, *J. Appl. Phys.* **71**, 1888-1892 (1992).
22. V.P. Koshelets, S.V. Shitov, A.V. Shchukin, L.V. Filippenko, I.L. Lapitskaya, and J. Mygind, *IEEE Trans. Appl. Supercond* (1995).